Journal of *Vascular Diseases*

MDPI

Article

Cerebral Arterial Inflow and Venous Outflow Assessment Using 4D Flow MRI in Adult and Pediatric Patients

Ramez N. Abdalla [1,2,3], Susanne Schnell [1], Maria Aristova [1], Mohamad Mohayad Alzein [1], Yasaman Moazeni [1], Jessie Aw [1,3], Can Wu [1,4], Michael Markl [1], Donald R. Cantrell [1,3], Michael C. Hurley [5], Sameer Ansari [1,3,5,6,7] and Ali Shaibani [1,3,5,6,7,*]

1 Department of Radiology, Neurology and Neurological Surgery, Feinberg School of Medicine, Northwestern University, 676 N. St. Clair Street, Suite 800, Chicago, IL 60611, USA; abdalla.r@northwestern.edu (R.N.A.); mmarkl@northwestern.edu (M.M.)
2 Department of Radiology, Faculty of Medicine, Ain Shams University, Cairo 11566, Egypt
3 Department of Radiology, Lurie Children's Hospital, Chicago, IL 60611, USA
4 Department of Medical Physics, Memorial Sloan Kettering Cancer Center, New York, NY 10065, USA
5 Department of Radiology, University of Chicago, Chicago, IL 60637, USA
6 Department of Neurological Surgery, Feinberg School of Medicine, Northwestern University, Chicago, IL 60208, USA
7 Department of Neurology, Feinberg School of Medicine, Northwestern University, Chicago, IL 60208, USA
* Correspondence: ashaibani@luriechildrens.org; Tel.: +1-312-695-5978; Fax: +1-312-695-4108

Abstract: Background and Purpose: The cerebral circulation is highly regulated to maintain brain perfusion, keeping an equilibrium between the brain tissue, cerebrospinal fluid (CSF) and blood of the arterial and venous systems. Cerebral venous drainage abnormalities have been implicated in multiple cerebrovascular diseases. The purpose of this study is to evaluate the relationship between the arterial inflow (AI) and the cerebral venous outflow (CVO) and their correlation with the cardiac outflow in healthy adults and children to understand the role of the emissary veins in normal venous drainage. Materials and Methods: A total of 31 healthy volunteers (24 adults (39.5 ± 16.0) and seven children (3.4 ± 2.2)) underwent intracranial 4D flow with full circle of Willis coverage and 2D PC-MRI at the level of the transverse sinus for measurement of the AI and CVO, respectively. The AI was calculated as the sum of the flow values in the bilateral internal carotid and basilar arteries. The CVO was calculated as the sum of the flow values in the bilateral transverse sinuses. The cardiac outflow was measured via 2D PC-MRI with retrospective ECG gating with images acquired at the proximal ascending aorta (AAo) and descending (DAo) aorta. The ratios of the AI/AAo flow and CVO/AI were calculated to characterize the fraction of cerebral arterial inflow in relation to cardiac outflow and venous blood draining through the transverse sinuses, respectively. Results: The AI and CVO were significantly correlated (r = 0.81, $p < 0.001$). The CVO constituted approximately 60–70% of the AI. The CVO/AI ratio was significantly lower in children versus adults ($p = 0.025$). In adults, the negative correlation of the AI with age remained strong (r = −0.81, $p < 0.001$). However, the CVO was not significantly associated with age. Conclusion: The CVO/AI ratio suggests an important role of the emissary veins, accounting for approximately 30–40% of venous drainage. The lower CVO/AI ratio in children, although partially related to decreased AI with age, suggests a greater role of the emissary veins in childhood, which strongly decreases with age.

Keywords: 4D flow; cerebral blood flow; cerebral veins; emissary veins; hemodynamics

Citation: Abdalla, R.N.; Schnell, S.; Aristova, M.; Alzein, M.M.; Moazeni, Y.; Aw, J.; Wu, C.; Markl, M.; Cantrell, D.R.; Hurley, M.C.; et al. Cerebral Arterial Inflow and Venous Outflow Assessment Using 4D Flow MRI in Adult and Pediatric Patients. *J. Vasc. Dis.* **2024**, *3*, 407–418. https://doi.org/10.3390/jvd3040032

Academic Editor: Ignatios Ikonomidis

Received: 28 August 2024
Revised: 3 November 2024
Accepted: 8 November 2024
Published: 13 November 2024

1. Introduction

The cerebral circulation is highly regulated to maintain satisfactory brain perfusion. In a healthy individual, several physiologic systems act to maintain adequate cerebral blood flow through modulation of a variety of parameters, including the arterial blood pressure, cerebral arterial and venous pressures, intracranial pressure, and cerebral vascular

resistance. These parameters contribute to maintaining a state of dynamic equilibrium between the cerebral blood flow, the cerebrospinal fluid volume, and the remaining major brain components. This is described by the Monro–Kellie doctrine, which states that the volumes of brain tissue, CSF, and blood consisting of the arterial and venous systems remain constant in a state of dynamic equilibrium with reciprocal compensation [1].

Therefore, the cerebral venous system plays an important role in intracranial hemodynamics and cerebral spinal fluid regulation, with a significant impact on the pathophysiological changes in intracranial pressures [2]. Abnormalities in the cerebral venous system and chronic cerebrospinal venous insufficiency have been implicated in a variety of neurological conditions, including multiple sclerosis, idiopathic intracranial hypertension and normal pressure hydrocephalus [3–5]. Despite these entities having different pathophysiological mechanisms, they may all share a relationship to venous stenosis/insufficiency. Consequently, understanding the normal blood flows across the arterial and venous systems, and how they correlate, is important to understand the underlying pathophysiology of the aforementioned diseases and their treatment.

Unfortunately, there is a significant paucity of studies investigating the venous cerebral hemodynamics in either normal or pathological states. What is widely appreciated is the gross cerebral venous anatomy and drainage that occurs via the superficial cortical and deep cerebral veins. This in turn drains into the dural venous sinuses, then through the internal jugular vein, posterior paraspinous, or perivertebral veins into the superior vena cava. In addition, there is some contribution of venous drainage through the extracranial veins, via the emissary veins [2].

Estimation of the total arterial cerebral blood flow and extracranial venous drainage has been described using color Doppler sonography (CDS) flow volume measurement [6,7]. However, CDS is operator-dependent and has low interobserver agreement [8]. In addition, it is limited to the assessment of the venous outflow in the extracranial veins, such as the internal jugular vein (IJV) and vertebral veins, while being unable to detect the dural venous sinuses and spinal epidural veins due to the inadequate temporal acoustic window, especially in adults [9,10], limiting the global assessment of the venous system.

Four-dimensional (4D) flow MRI is a quantitative technique that has been widely used for the assessment of 4D blood flow in a number of complex intracerebral lesions, such as intracranial stenosis, aneurysms, arteriovenous malformations (AVMs), and investigation of normal hemodynamic states in healthy volunteers [11–13]. Moreover, 4D flow MRI can provide the net flow, total flow, peak velocities, and advanced hemodynamic parameters. The wall shear stress or pressure gradients can be derived, and it is currently being studied in the major vessels [14].

A prior study investigating age-related changes in the normal cerebral and cardiac output in children and adults provides the impetus for the current work [15]. The successful use of 2D and 4D flow MRI has been described previously for in vivo assessment and quantification of the physiologic blood flow in the intracranial veins in healthy volunteers and multiple sclerosis patients [16–20]. However, to the best of our knowledge, there are no published studies quantifying the relationship between the normal cerebral arterial inflow and the venous outflow using 4D flow MRI. According to the Monro–Kellie doctrine, the venous outflow should be either equal or slightly increased in comparison to the cerebral blood flow due to CSF resorption into the dural venous sinuses. The goal of this work is to quantitatively study the relationship between the arterial inflow and the venous outflow in the cerebral circulation in healthy adult and pediatric volunteers, to highlight any age discrepancies, and to determine the role of the emissary veins in cerebral venous drainage.

2. Methods and Materials

2.1. Participants

The study population consisted of 31 healthy volunteers who underwent brain MRI, including 4D flow MR imaging and CINE phase-contrast MRI (PC-MRI), in a previous study. Patients without venous outflow measurements were excluded [15]. This group consisted

of 24 adults (12 females, age 39.5 ± 16.0 years, [range 19.2–60.7]) and 7 children (3 females, age 3.4 ± 2.2 years, [range 0.9–7.2]). Subjects were screened for factors that would influence the blood flow parameters, including a history of cardiac and cerebrovascular disease, blood pressure, and ECGs. Subjects with a BMI > 35 kg/m^2, a blood pressure > 160/90, and a history of cardiac or cerebrovascular disease, liver or renal disorder, brain surgery, smoking or drug abuse were excluded. The study protocol was approved by the Institutional Review Board and the study was conducted in accordance with the Health Insurance Portability and Accountability Act guidelines. Written informed consent was obtained from all the adults and from the children's parents or legal guardians prior to participation in the study.

2.2. Data Acquisitions and MRI Protocol

All the MRI exams were performed on a 3 Tesla MAGNETOM Skyra MRI (Siemens Healthcare, Erlangen, Germany). The participants were scanned in the supine position and children under 6 years old were scanned under anesthesia or sedation.

2.2.1. Cerebral Arterial Inflow

Four-dimensional flow MRI was acquired with volumetric coverage of the major cerebral arteries to measure the cerebral arterial inflow. Figure 1A illustrates the volume coverage and location of selected planes used for the assessment of the cerebral arterial inflow. Four-dimensional flow MRI was acquired with a time-resolved ECG-gated (CINE) three-dimensional (3D) phase-contrast (PC) MRI with velocity encoding along three spatial directions (Vx, Vy, and Vz) [21–25]. Initially, 3D axial time-of-flight magnetic resonance angiography (MRA) was performed to set up the 4D flow imaging coverage. The flow component of the acquisition was prospectively ECG-gated and accelerated using GRAPPA R = 2. The MR sequence parameters were as follows: echo time, TE = 2.8–3.2 ms; repetition time, TR = 5.2–5.6 ms; temporal resolution = 41.6–44.8 ms; flip angle, FA = 15°; in-plane resolution = (1.1 − 1.2) × (1.1 − 1.2) mm^2, and slice thickness = 1.2–1.4 mm. In the original study, the peak velocities in the MCAs were 0.98 ± 0.26 and 0.71 ± 0.17 m/s for children and adults, respectively, and reached a maximum at ~6 years [15]. Therefore, the velocity encoding sensitivity was set to 80 cm/s for adults, children < 4 years, and children > 8 years, and 100 cm/s was used for children 4–8 years (Table 1). All the datasets were acquired successfully with a 4D Flow MRI acquisition time of 8–20 min, depending on the volunteer's heart rate.

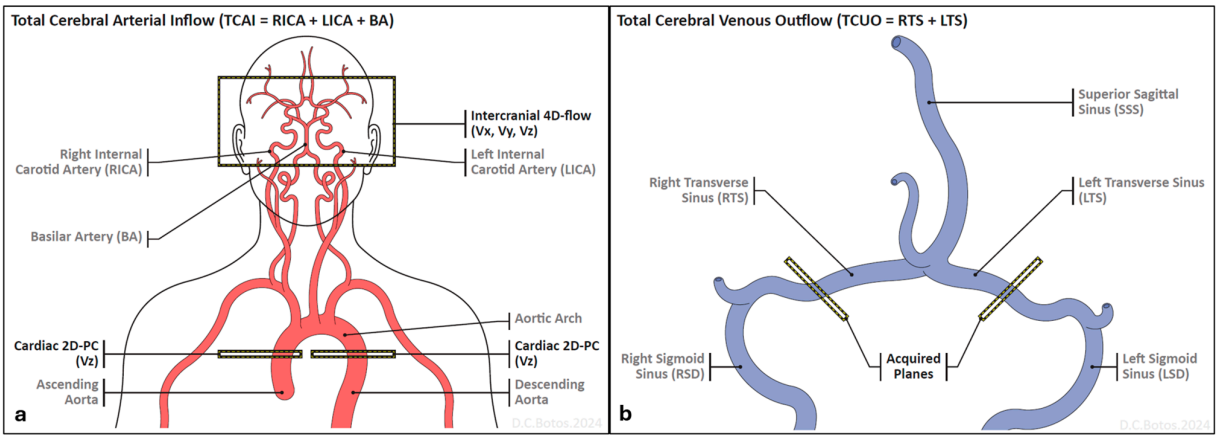

Figure 1. (**a**) Diagram depicting the locations utilized for the total cerebral arterial inflow analysis at the supra-clinoid internal carotid arteries and distal basilar artery, as well as the cardiac outflow analysis. (**b**) Diagram depicting the planes acquired for the total cerebral venous outflow analysis at the left and right transverse sinuses.

Table 1. Pulse sequence parameters for the 4D flow and 2D phase-contrast MRI.

Sequence Parameters	Flow Sequences		
	4D Flow MRI (3-Directional)	**2D PC-MRI (TS) (Through-Plane)**	**2D PC-MRI (Aorta) (Through-Plane)**
TR/TE (ms)	5.2/2.8	4.6/2.4	4.6/2.4
Flip Angle (°)	15	30	30
VENC (cm/s)	80–100	50	150
Voxel Size (mm^3)	1.2 × 1.2 × 1.4	1.2 × 1.2 × 6.0	1.2 × 1.2 × 7.0
Temporal Resolution (ms)	42	28	28
Acquisition Time	8–20 min	12–22 s	12–22 s
Respiration	Free-breathing	Free-breathing	Breath-hold (adults)
ECG Gating	Prospective	Retrospective	Retrospective

Note: TS = transverse sinus, VENC = velocity encoding.

2.2.2. Cerebral Venous Outflow

Two standard two-dimensional phase-contrast (2D PC)-MRI scans with retrospective ECG gating were acquired at two anatomical positions with through-plane velocity encoding: at the left and right distal transverse sinuses to measure the cerebral outflow (Figure 1B). The imaging parameters for the through-plane PC-MRI in the transverse sinuses were TE = 2.4–2.6 ms; TR = 4.6–4.65 ms; temporal resolution = 27.7–27.9 ms, 30-degree flip angle, in-plane resolution = 1.2 × 1.2 mm^2; and 6 mm slice thickness. The velocity encoding sensitivity was set at 50 cm/s (Table 1).

2.2.3. Cardiac Outflow

Two standard two-dimensional phase-contrast (2D PC)-MRI scans with retrospective ECG gating were acquired at two anatomical positions with through-plane velocity encoding: at the proximal ascending aorta (AAo) and descending aorta (DAo) distal to the origin of the major vessels of the head and neck (Figure 1A). The imaging parameters for the through-plane PC-MRI in the aorta were TE = 2.4–2.6 ms; TR = 4.6–4.65 ms; temporal resolution = 27.7–27.9 ms, 30-degree flip angle, in-plane resolution = 1.2 × 1.2 mm^2; and 7 mm slice thickness. The velocity encoding sensitivity was set at 150 cm/s (Table 1).

2.3. Data Analysis

The 4D flow MRI data were preprocessed using in-house software tools programed in MATLAB (The MathWorks, Natick, MA, USA). The 4D flow data preprocessing involved correction for background noise, phase offset errors due to the eddy current, and velocity antialiasing according to previously reported strategies [26]. In addition, a 3D phase-contrast angiogram (PC-MRA) was calculated using the pseudo-complex difference method and used in the following steps for masking the velocities within the vessel boundaries, as previously described [27,28]. Next, the preprocessed 4D flow MRI data were loaded into a commercial 3D visualization software package (EnSight, CEI, Apex, NC, USA). Based on the 3D PC-MRA data, 2D analysis planes were manually placed within the 3D volume at the left and right internal carotid arteries (LICA, RICA) and the basilar artery (BA). Based on the 3D PC-MRA vessel controls, the blood flow was quantified at all the 2D analysis plane locations. Analysis of the 2D PC MRI data included the manual delineation of the vessel lumen contours for all the time frames across the cardiac cycle using a dedicated flow analysis tool (Argus, Siemens, Germany). The final contours were used to calculate the vessel areas, mean velocity, net and peak flow, as well as peak velocity.

The mean blood flow parameters (expressed in mL/s) were calculated at the cerebral levels in the supra-clinoid segment of the bilateral internal carotid arteries, basilar artery and transverse sinuses (Figure 1). The cerebral arterial inflow (mL/s) was calculated as the cumulative flow/sum of the inflow of the bilateral internal carotid arteries (ICAs) and basilar artery (BA) (Figure 1A). The cerebral venous outflow (mL/s) was calculated as the cumulative/sum of the venous outflow in the bilateral transverse sinuses (Figure 1B). The

ratios of cerebral venous outflow to arterial inflow, cerebral arterial inflow to aortic outflow, and ascending aortic outflow to descending aortic outflow were calculated.

2.4. Statistical Analysis

All the flow parameters were expressed as the mean ± SD. Using a univariate analysis with a nonparametric Mann–Whitney test, the ratios of the cerebral venous outflow and arterial inflows were compared between adults and children. The cerebral and cardiac flow parameters (AI, CVO and AI/AAo) were plotted against age and fitted using regression. The CVO was also plotted against the AI and fitted using linear regression. The level for statistical significance (p-value) was set at 0.05. The nonparametric Spearman coefficient test was used to determine if there was a correlation between the flow parameters and age (correlation coefficient r and p-values were reported). Statistical analysis for this paper was performed using the Real Statistics Resource Pack software (Release 4.3, Copyright (2013–2015) Charles Zaiontz, www.real-statistics.com, accessed on 28 August 2024).

3. Results

Intracranial and cardiac data were successfully acquired, and flow analysis was successfully performed for all the participants. The cerebral arterial inflow and cerebral venous outflow were calculated for the entire cohort. Subgroup analysis was performed to compare the flow parameters between children and adults and to identify the relationship between the flow parameters and age (Table 2).

Table 2. Summary of subject characteristics and flow parameters.

	Subject Subgroups		p-Values
	Children	**Adults**	
Subject Characteristics			
Number	7	24	
Mean Age (years)	3.4 ± 2.2	39.5 ± 16.0	
Age Range (years)	0.9–7.2	19.2–60.7	
Gender (male/female)	4/3	12/12	
Cerebral Flow Parameters			
LICA (mL/s)	7.36 ± 1.54	4.44 ± 0.76	<0.001 *
RICA (mL/s)	7.37 ± 1.98	4.54 ± 1.04	<0.001 *
BA (mL/s)	5.47 ± 1.70	2.80 ± 0.86	<0.001 *
Cerebral Arterial Inflow (mL/s)	20.21 ± 4.58	11.78 ± 2.03	<0.001 *
Left Transverse Sinus (mL/s)	6.02 ± 3.47	3.72 ± 2.68	0.072
Right Transverse Sinus (mL/s)	6.79 ± 1.76	5.31 ± 2.98	0.226
Cerebral Venous Outflow (mL/s)	12.80 ± 3.82	9.03 ± 2.31	0.003 *
Cardiac Flow Parameters			
AAo (mL/s)	46.52 ± 13.98	81.39 ± 14.31	<0.001 *
DAo (mL/s)	16.74 ± 7.38	53.09 ± 11.68	<0.001 *
Flow Relationships (Flow Ratios)			
Cerebral V-Outflow/A-Inflow	0.63 ± 0.11	0.76 ± 0.14	0.025 *
Cerebral A-Inflow/AAo flow	0.45 ± 0.08	0.15 ± 0.02	<0.001 *
Relationship with Age (Spearman's Correlation Coefficient r and p-value)			
Cerebral Arterial Inflow vs. Age	r = 0.71, p = 0.072	r = −0.69, p < 0.001 *	
Cerebral Venous Outflow vs. Age	r = 0.89, p = 0.007 *	r = −0.29, p = 0.171	
V-Outflow/A-Inflow vs. Age	r = 0.31, p = 0.504	r = 0.16, p = 0.446	
Cerebral A-Inflow/AAo flow vs. Age	r= −0.36, p = 0.432	r = −0.35, p = 0.095	

Note: V-Outflow = cerebral venous outflow, A-Inflow = cerebral arterial inflow, * indicates significant difference or association with p-value < 0.05, ICA = internal carotid artery, L = left, R = right, BA = basilar artery.

3.1. Cerebral Arterial Inflow

The cerebral arterial inflow (20.21 ± 4.58 mL/s versus 11.78 ± 2.03 mL/s; $p < 0.001$) was significantly higher in children compared to adult volunteers (Table 2). There was a trend toward increased cerebral arterial inflow from birth to the age of 8 years (r = 0.71, $p = 0.072$) (Figure 2A), then there was a significant decrease in the cerebral arterial inflow from the age of 19 onwards (r = −0.69, $p < 0.001$) (Table 2 and Figure 3A). In the combined cohort of children and adults, the cerebral arterial inflow (r = −0.81, $p < 0.001$) correlated negatively with age (Figure 4A).

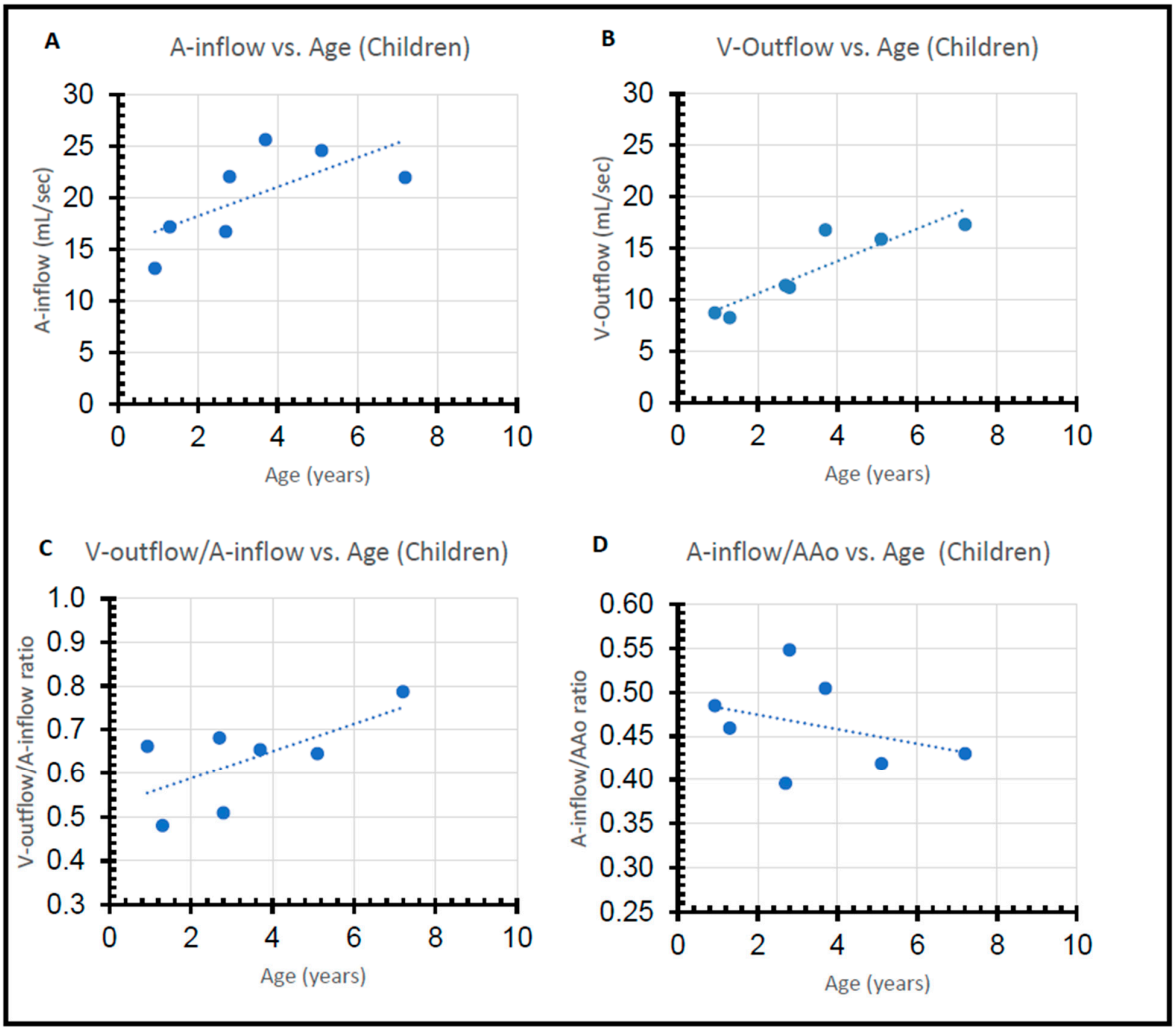

Figure 2. Age-related trends of cerebral inflow and outflow in children. (**A**) Age-related arterial inflow, (**B**) age-related venous outflow, (**C**) age-related outflow/inflow ratio, and (**D**) age-related inflow/AAo ratio.

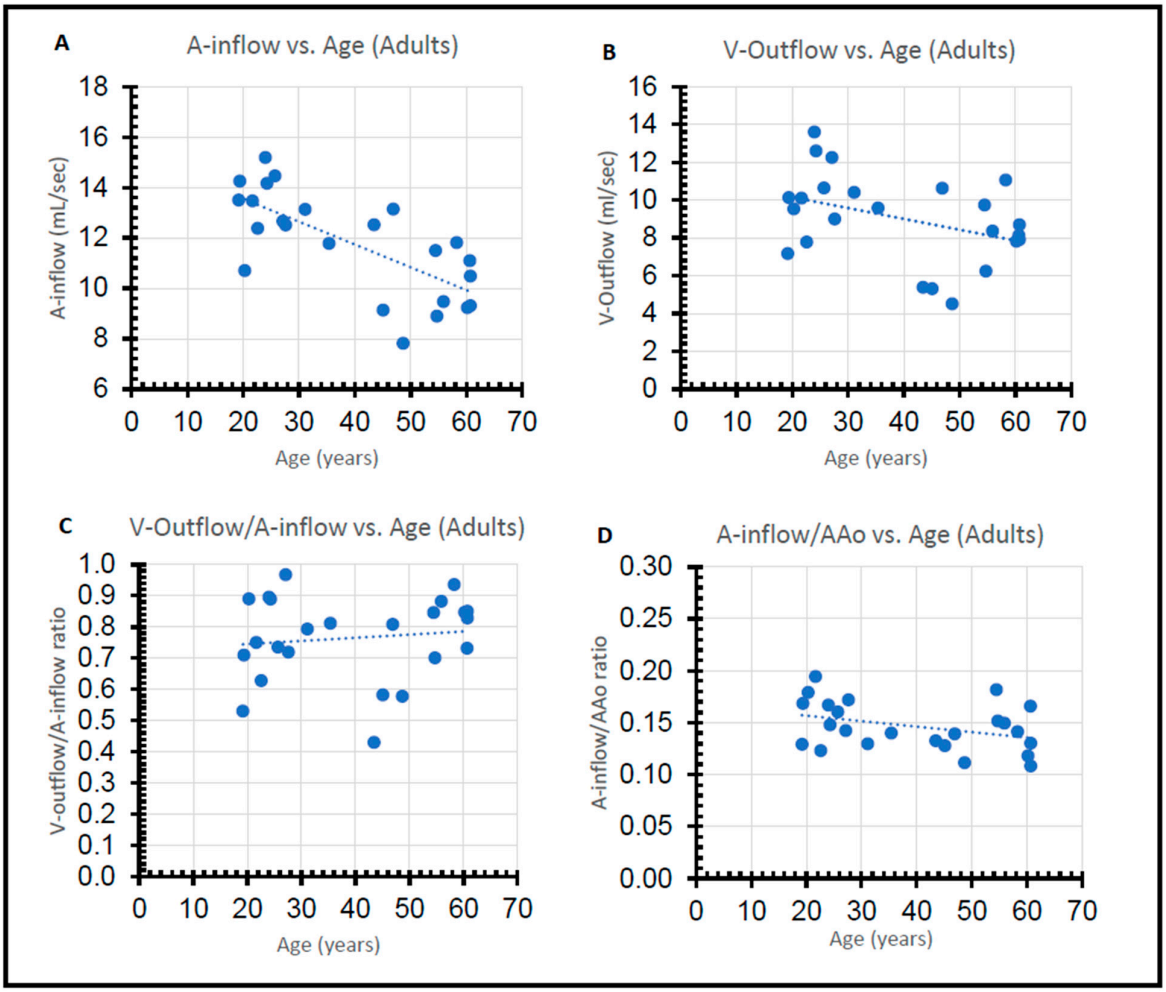

Figure 3. Age-related trends of cerebral inflow and outflow in adults. (**A**) Age-related arterial inflow, (**B**) age-related venous outflow, (**C**) age-related outflow/inflow ratio, and (**D**) age-related inflow/AAo ratio.

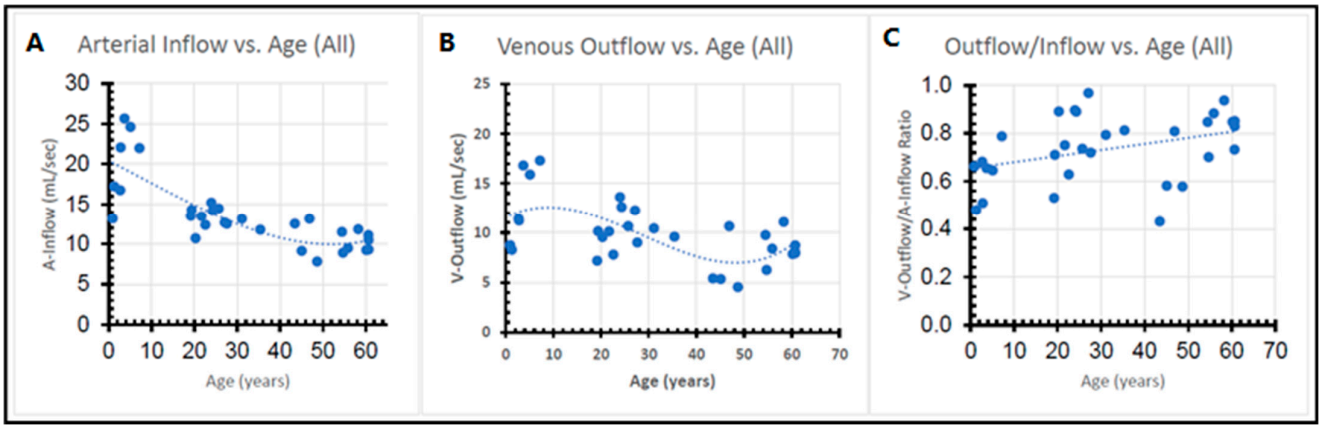

Figure 4. General trends of (**A**) the arterial inflow, (**B**) the venous outflow, and (**C**) the ratio of venous outflow to arterial inflow in the entire cohort.

3.2. Cerebral Venous Outflow

The cerebral venous outflow (12.80 ± 3.82 mL/s versus 9.03 ± 2.31 mL/s; $p = 0.003$) was significantly higher in children compared to adult volunteers (Table 2). The cerebral venous outflow increased significantly from birth until the age of 7 years (r = 0.89, $p = 0.007$)

(Figure 2B), then decreased slowly from 19 years onwards (r = −0.29, $p = 0.171$) (Table 2 and Figure 3B). In the combined cohort of children and adults, the cerebral venous outflow (r = −0.44, $p = 0.012$) correlated negatively with age (Figure 4B).

3.3. Cerebral Venous Outflow/Cerebral Arterial Inflow Ratio and Correlation with Age

The CVO increased significantly with increased AI (r = 0.81 and $p < 0.001$) in the entire cohort (Figure 5A). The ratio of the mean cerebral venous outflow to the arterial inflow (CVO/AI) was significantly higher in adult volunteers when compared to children (0.63 ± 0.01 versus 0.76 ± 0.02, $p = 0.025$) (Table 2 and Figure 5). However, there was no significant linear correlation between the outflow/inflow ratio and age in adults (r = −0.35, $p = 0.095$) or children (r = −0.36, $p = 0.432$) (Figures 2C and 3C, respectively).

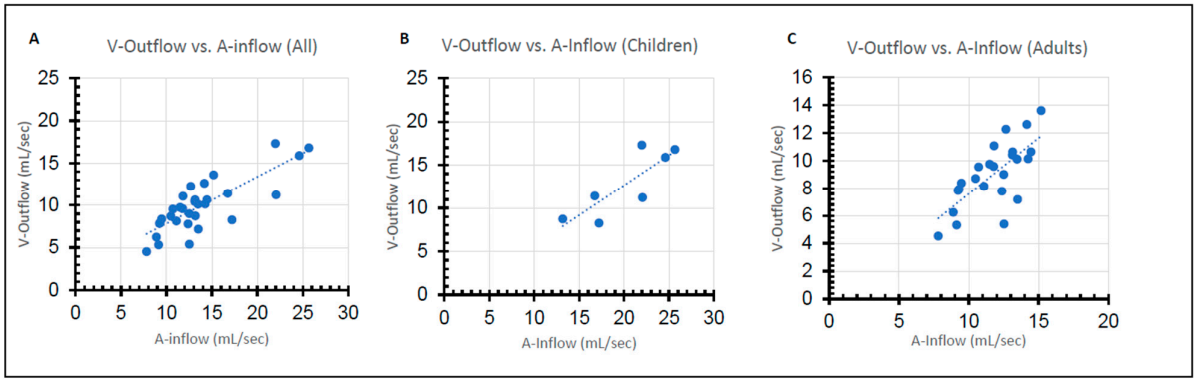

Figure 5. Linear correlation between the arterial inflow and venous outflow for the (**A**) entire cohort, (**B**) children, and (**C**) adults.

The systemic aortic outflow (AAo) and descending aortic outflow (DAo) were significantly higher in adults (81.4 vs. 46.5 mL/s; $p < 0.001$ and 53.1 vs. 16.8; $p < 0.001$, respectively). The mean difference between the systemic aortic outflow and descending aortic outflow was not significantly different between adults and children (29.8 vs. 28.4 mL/s; $p = 0.67$).

4. Discussion

The cerebral venous outflow, as a percentage of the arterial inflow, was analyzed in healthy adults and children using 4D flow MRI techniques. A strong positive correlation between the CVO and the AI was observed for the entire cohort. This correlation persisted in both the adult and the pediatric cohorts. The cerebral AI and CVO were significantly higher in children when compared to adults and correlated negatively with age. However, the ratio of CVO/AI was significantly lower in children compared to adults, which could in part be related to the decreases AI in adults. However, the higher inflow in children and lower CVO/AI ratio are also suggestive of age-related changes in the pathways of venous drainage and a more important role for emissary vein utilization in childhood.

Flow quantification of the dural venous sinuses utilizing 2D phase-contrast magnetic resonance imaging (2D PC-MRI) has been studied in the past in healthy volunteers, patients with normal pressure hydrocephalus, idiopathic intracranial hypertension, and in children with achondroplasia [29–34]. On the one hand, 2D PC-MRI-based measurements of the velocity and flow within the major cerebral venous sinuses focused on the superior sagittal sinus, while flow quantification in the smaller cerebral sinuses was limited due to the small size variability and tortuosity of the veins. On the other hand, 4D flow MRI has recently been used to study the physiologic flow in the superficial dural veins due to its high spatial and temporal resolution [16]. Moreover, 4D flow MRI techniques with 3D visualization of the blood flow and retrospective quantification of the velocity at any given point within the vessel allow for comprehensive evaluation of the complex blood flow patterns and a

more detailed quantification of hemodynamic parameters such as the total cerebral in- and outflow, flow rate, and peak velocity [16,35].

The brain AI is mainly provided by the internal carotid arteries and the vertebrobasilar system. On the other hand, venous drainage of the brain shows greater variation. However, it can be simplified into supratentorial venous drainage by the superficial and deep (subependymal and medullary) cerebral veins and infratentorial drainage via the bridging veins (draining posterior fossa). Both eventually drain into the dural venous sinuses and subsequently to the IJV and vertebral/paraspinous veins, constituting the main drainage pathway for the intracranial circulation in the supine and upright positions, respectively [2]. Another important pathway for cerebral venous drainage is through the emissary and diploic veins, connecting meningeal veins and dural sinuses to the scalp and extracranial venous plexuses [36].

The postural dependence of the CVO has been described, with the IJV being the principal outflow for intracranial blood in the supine position. In the seated and erect position, the IVJ collapses in, shifting the blood flow to the vertebral veins with a contribution from the spinal epidural veins, condylar veins, as well as occipital and mastoid emissary veins connecting the posterior cranial fossa dural venous sinuses to the vertebral venous system [7,37,38].

Although the role of the emissary veins and the vertebral venous plexus has previously been described, to the best of our knowledge, no studies have addressed the relative percentage of the CVO through different drainage pathways, including the emissary veins, which could have implications for the assessment and pathophysiology of several diseases. In our study, 76% of the AI entering the brain in adults was drained through the transverse sinus. This suggests that approximately 24% of the venous drainage in the supine position is directed through the emissary and condylar veins to the extracranial venous. The role of the emissary veins is greater in the pediatric population, as only 63% of the cerebral AI is drained through the transverse/sigmoid junction. As a result, approximately one-third of the venous outflow in the pediatric age group in the supine position is being directed through the emissary and condylar veins. The differences between the adult and the pediatric age groups could be due to increased intracranial venous drainage development in adults, leading to greater capacity and decreased reliance on extracranial drainage. Another explanation could be due to the higher cerebral inflow in the pediatric age group, which constitutes approximately 45% of the aortic outflow compared to 14% in adults. Therefore, an increased contribution of extracranial venous drainage would be required to compensate for the increased flow.

4.1. Limitations

The present study is not without limitations. First, the study cohort is limited in size. Therefore, some of the discrepancies between children and adults may be due to the small number of children recruited. Additionally, previous studies have shown the occipital sinus to be present in children up to the age of 9 years, especially in the first 2 years of life. Its disappearance/hypoplasia has been attributed to a shift in the pattern of venous drainage from predominantly the IJV during infancy to the internal and external vertebral venous plexus as children learn to walk. This might have caused the significantly lower outflow through the transverse/sigmoid junction in our pediatric cohort [39]. However, after analyzing the structural/anatomic imaging, none of our pediatric subjects were found to have had an occipital sinus. Another limitation of our study is the lack of validation of the 4D flow results with different imaging modalities in the subjects evaluated. However, previous studies have demonstrated that 4D flow MRI accurately assesses the blood velocities in the extracranial circulation with mild over- and underestimation of high and low velocities, respectively [16,40]. Doppler assessment is restricted by the bone window at the intracranial portion of the carotid and basilar arteries, as well as the transverse/sigmoid junction, making it inadequate for flow assessment at those locations. Lastly, the mean flow parameters were sampled at the level of the supraclinoid ICAs and

basilar arteries, which excludes the AI through the posterior inferior cerebellar arteries. However, the CVO was also determined at the level of the transverse/sigmoid junction, excluding the venous drainage from the inferior petrosal sinus, likely compensating for the missed AI.

4.2. Conclusions

To the best of our knowledge, the current study is the first to quantify the amount of cerebral venous outflow relative to the arterial inflow in adult and pediatric populations. Our study suggests an important role of the emissary veins in cerebral venous drainage in the supine position, contributing to at least one-third and one-fourth of the venous outflow in the pediatric and adult populations, respectively. This may be suggestive of the important role these drainage pathways may play in the pathophysiology of diseases related to chronic venous insufficiency. Further studies to assess the amount of CVO carried by the emissary veins in patients with diseases such as multiple sclerosis and pseudotumor cerebri could pave the way for better understanding and management of such diseases.

Author Contributions: All the authors of this manuscript have contributed to the work as per the following ICMJE recommendations: "Substantial contributions to the conception or design of the work, or the acquisition, analysis or interpretation of data. Drafting the work or revising it critically for important intellectual content. Final approval of the version published. Agreement to be accountable for all aspects of the work in ensuring that questions related to the accuracy or integrity of any part of the work are appropriately investigated and resolved". A.S. is the guarantor of the manuscript and conceptualized the work. A.S., R.N.A., S.S., J.A., M.A., Y.M. and M.M.A. performed the literature search and/or contributed to writing the manuscript. A.S., S.A., M.C.H., D.R.C., M.M., C.W., S.S. and M.A. identified and managed the cases, performed the procedures, and contributed to editing the manuscript. All authors have read and agreed to the published version of the manuscript.

Funding: NIH F30 HL140910 (Aristova), NIH T32 GM815229 (Northwestern). American Heart Association (AHA) Predoctoral Fellowship 14PRE18370014, Radiological Society of North America (RSNA) Research Seed Grant RSD1207.

Institutional Review Board Statement: This study was approved by the Northwestern University Institutional Review Board, with IRB number: STU00207590.

Informed Consent Statement: A consent waiver was obtained due to the retrospective nature of the study with no deviation from the standard clinical practice.

Data Availability Statement: Data are contained within the article.

Conflicts of Interest: The authors declare no conflict of interest.

References

1. Mokri, B. The Monro-Kellie hypothesis: Applications in CSF volume depletion. *Neurology* **2001**, *56*, 1746–1748. [CrossRef] [PubMed]
2. Schaller, B. Physiology of cerebral venous blood flow: From experimental data in animals to normal function in humans. *Brain Res. Rev.* **2004**, *46*, 243–260. [CrossRef] [PubMed]
3. Zamboni, P.; Galeotti, R.; Menegatti, E.; Malagoni, A.M.; Tacconi, G.; Dall'Ara, S.; Bartolomei, I.; Salvi, F. Chronic cerebrospinal venous insufficiency in patients with multiple sclerosis. *J. Neurol. Neurosurg. Psychiatry* **2008**, *80*, 392–399. [CrossRef] [PubMed]
4. Karahalios, D.G.; Rekate, H.L.; Khayata, M.H.; Apostolides, P.J. Elevated intracranial venous pressure as a universal mechanism in pseudotumor cerebri of varying etiologies. *Neurology* **1996**, *46*, 198–202. [CrossRef] [PubMed]
5. Bateman, G.A. The Pathophysiology of Idiopathic Normal Pressure Hydrocephalus: Cerebral Ischemia or Altered Venous Hemodynamics? *AJNR Am. J. Neuroradiol.* **2008**, *29*, 198–203. [CrossRef]
6. Schöning, M.; Walter, J.; Scheel, P. Estimation of cerebral blood flow through color duplex sonography of the carotid and vertebral arteries in healthy adults. *Stroke* **1994**, *25*, 17–22. [CrossRef]
7. Schreiber, S.J.; Lürtzing, F.; Götze, R.; Doepp, F.; Klingebiel, R.; Valdueza, J.M. Extrajugular pathways of human cerebral venous blood drainage assessed by duplex ultrasound. *J. Appl. Physiol.* **2003**, *94*, 1802–1805. [CrossRef]
8. Laukontaus, S.J.; Kagayama, T.; Lepäntalo, M.; Atula, S.; Färkkilä, M.; Albäck, A.; Inoue, Y.; Tienari, P.; Venermo, M. Doppler Ultrasound Examination of Multiple Sclerosis Patients and Control Participants: Inter-observer Agreement and Association with Disease. *Eur. J. Vasc. Endovasc. Surg.* **2013**, *46*, 466–472. [CrossRef]

9. Kassab, M.Y.; Majid, A.; Farooq, M.U.; Azhary, H.; Hershey, L.A.; Bednarczyk, E.M.; Graybeal, D.F.; Johnson, M.D. Transcranial Doppler: An Introduction for Primary Care Physicians. *J. Am. Board Fam. Med.* **2007**, *20*, 65–71. [CrossRef]
10. Stolz, E.; Kaps, M.; Dorndorf, W. Assessment of Intracranial Venous Hemodynamics in Normal Individuals and Patients With Cerebral Venous Thrombosis. *Stroke* **1999**, *30*, 70–75. [CrossRef]
11. Ansari, S.A.; Schnell, S.; Carroll, T.; Vakil, P.; Hurley, M.C.; Wu, C.; Carr, J.; Bendok, B.R.; Batjer, H.; Markl, M. Intracranial 4D Flow MRI: Toward Individualized Assessment of Arteriovenous Malformation Hemodynamics and Treatment-Induced Changes. *AJNR Am. J. Neuroradiol.* **2013**, *34*, 1922–1928. [CrossRef] [PubMed]
12. Hope, T.A.; Hope, M.D.; Purcell, D.D.; von Morze, C.; Vigneron, D.B.; Alley, M.T.; Dillon, W.P. Evaluation of intracranial stenoses and aneurysms with accelerated 4D flow. *Magn. Reson. Imaging* **2010**, *28*, 41–46. [CrossRef] [PubMed]
13. Hope, M.D.; Purcell, D.D.; Hope, T.A.; Von Morze, C.; Vigneron, D.B.; Alley, M.T.; Dillon, W.P. Complete Intracranial Arterial and Venous Blood Flow Evaluation with 4D Flow MR Imaging. *AJNR Am. J. Neuroradiol.* **2009**, *30*, 362–366. [CrossRef] [PubMed]
14. Markl, M.; Wallis, W.; Harloff, A. Reproducibility of flow and wall shear stress analysis using flow-sensitive four-dimensional MRI. *Magn. Reson. Imaging* **2011**, *33*, 988–994. [CrossRef] [PubMed]
15. Wu, C.; Honarmand, A.R.; Schnell, S.; Kuhn, R.; Schoeneman, S.E.; Ansari, S.A.; Carr, J.; Markl, M.; Shaibani, A. Age-Related Changes of Normal Cerebral and Cardiac Blood Flow in Children and Adults Aged 7 Months to 61 Years. *J. Am. Heart Assoc.* **2016**, *5*, e002657. [CrossRef]
16. Schuchardt, F.; Schroeder, L.; Anastasopoulos, C.; Markl, M.; Bäuerle, J.; Hennemuth, A.; Drexl, J.; Valdueza, J.M.; Mader, I.; Harloff, A. In vivo analysis of physiological 3D blood flow of cerebral veins. *Eur. Radiol.* **2015**, *25*, 2371–2380. [CrossRef]
17. Wattjes, M.P.; Van Oosten, B.W.; De Graaf, W.L.; Seewann, A.; Bot, J.C.; Van Den Berg, R.; Uitdehaag, B.M.; Polman, C.H.; Barkhof, F. No association of abnormal cranial venous drainage with multiple sclerosis: A magnetic resonance venography and flow-quantification study. *J. Neurol. Neurosurg. Psychiatry* **2011**, *82*, 429–435. [CrossRef]
18. ElSankari, S.; Balédent, O.; van Pesch, V.; Sindic, C.; de Broqueville, Q.; Duprez, T. Concomitant Analysis of Arterial, Venous, and CSF Flows using Phase-Contrast MRI: A Quantitative Comparison Between MS Patients and Healthy Controls. *J. Cereb. Blood Flow Metab.* **2013**, *33*, 1314–1321. [CrossRef]
19. Schrauben, E.M.; Kohn, S.; Macdonald, J.; Johnson, K.M.; Kliewer, M.; Frost, S.; Fleming, J.O.; Wieben, O.; Field, A. Four-dimensional flow magnetic resonance imaging and ultrasound assessment of cerebrospinal venous flow in multiple sclerosis patients and controls. *J. Cereb. Blood Flow Metab.* **2017**, *37*, 1483–1493. [CrossRef]
20. Schuchardt, F.F.; Kaller, C.P.; Strecker, C.; Lambeck, J.; Wehrum, T.; Hennemuth, A.; Anastasopoulos, C.; Mader, I.; Harloff, A. Hemodynamics of cerebral veins analyzed by 2d and 4d flow mri and ultrasound in healthy volunteers and patients with multiple sclerosis. *Magn. Reson. Imaging* **2020**, *51*, 205–217. [CrossRef]
21. Moran, P.R. A flow velocity zeugmatographic interlace for NMR imaging in humans. *Magn. Reson. Imaging* **1982**, *1*, 197–203. [CrossRef] [PubMed]
22. Firmin, D.N.; Nayler, G.L.; Kilner, P.J.; Longmore, D.B. The application of phase shifts in NMR for flow measurement. *Magn. Reson. Med.* **1990**, *14*, 230–241. [CrossRef] [PubMed]
23. Wigström, L.; Sjöqvist, L.; Wranne, B. Temporally resolved 3D phase-contrast imaging. *Magn. Reson. Med.* **1996**, *36*, 800–803. [CrossRef]
24. Markl, M.; Chan, F.P.; Alley, M.T.; Wedding, K.L.; Draney, M.T.; Elkins, C.J.; Parker, D.W.; Wicker, R.; Taylor, C.A.; Herfkens, R.J.; et al. Time-resolved three-dimensional phase-contrast MRI. *Magn. Reson. Imaging* **2003**, *17*, 499–506. [CrossRef]
25. Markl, M.; Harloff, A.; Bley, T.A.; Zaitsev, M.; Jung, B.; Weigang, E.; Langer, M.; Hennig, J.; Frydrychowicz, A. Time-resolved 3D MR velocity mapping at 3T: Improved navigator-gated assessment of vascular anatomy and blood flow. *Magn. Reson. Imaging* **2007**, *25*, 824–831. [CrossRef]
26. Bock, J.; Kreher, B.W.; Hennig, J.; Markl, M. Optimized pre-processing of time-resolved 2D and 3D phase contrast MRI data. In Proceedings of the 15th Annual Meeting of ISMRM, Berlin, Germany, 19–25 May 2007; Volume 3138.
27. Schnell, S.; Ansari, S.A.; Vakil, P.; Wasielewski, M.; Carr, M.L.; Hurley, M.C.; Bendok, B.R.; Batjer, H.; Carroll, T.J.; Carr, J.; et al. Three-dimensional hemodynamics in intracranial aneurysms: Influence of size and morphology. *Magn. Reson. Imaging* **2014**, *39*, 120–131. [CrossRef]
28. Bock, J.; Wieben, O.; Johnson, K.M.; Hennig, J.; Markl, M. Optimal processing to derive static PC-MRA from time-resolved 3D PC-MRI data. *Imaging* **2007**, *25*, 824–831.
29. Mehta, N.R.; Jones, L.; Kraut, M.A.; Melhem, E.R. Physiologic Variations in Dural Venous Sinus Flow on Phase-Contrast MR Imaging. *Am. J. Roentgenol.* **2000**, *175*, 221–225. [CrossRef]
30. Enzmann, D.R.; Ross, M.R.; Marks, M.P.; Pelc, N.J. Blood Flow in Major Cerebral Arteries Measured by Phase-Contrast Cine MR. *AJNR Am. J. Neuroradiol.* **1994**, *15*, 123–129.
31. Jordan, J.E.; Pelc, N.J.; Enzmann, D.R. Velocity and flow quantitation in the superior sagittal sinus with ungated and cine (gated) phase-contrast MR imaging. *Magn. Reson. Imaging* **1994**, *4*, 25–28. [CrossRef]
32. Marks, M.P.; Pelc, N.J.; Ross, M.R.; Enzmann, D.R. Determination of cerebral blood flow with a phase-contrast cine MR imaging technique: Evaluation of normal subjects and patients with arteriovenous malformations. *Radiology* **1992**, *182*, 467–476. [CrossRef] [PubMed]

33. Gideon, P.; Thomsen, C.; Gjerris, F.; Sørensen, P.S.; Ståhlberg, F.; Henriksen, O. Measurement of blood flow in the superior sagittal sinus in healthy volunteers, and in patients with normal pressure hydrocephalus and idiopathic intracranial hypertension with phase-contrast cine MR imaging. *Acta Radiol.* **1996**, *37*, 171–176. [CrossRef] [PubMed]
34. Hirabuki, N.; Watanabe, Y.; Mano, T.; Fujita, N.; Tanaka, H.; Ueguchi, T.; Nakamura, H. Quantitation of Flow in the Superior Sagittal Sinus Performed with Cine Phase-contrast MR Imaging of Healthy and Achondroplastic Children. *AJNR Am. J. Neuroradiol.* **2000**, *21*, 1497–1501. [PubMed]
35. Markl, M.; Schnell, S.; Wu, C.; Bollache, E.; Jarvis, K.; Barker, A.; Robinson, J.; Rigsby, C. Advanced flow MRI: Emerging techniques and applications. *Clin. Radiol.* **2016**, *71*, 779–795. [CrossRef]
36. Byrne, J.V. *Tutorials in Endovascular Neurosurgery and Interventional Neuroradiology*; Springer International Publishing: Cham, Switzerland, 2017. [CrossRef]
37. Manuel Valdueza, J.; Von Münster, T.; Hoffman, O.; Schreiber, S.; Max Einhäupl, K. Postural dependency of the cerebral venous outflow. *Lancet* **2000**, *355*, 200–201. [CrossRef]
38. Ruíz, D.S.M.; Gailloud, P.; Rüfenacht, D.A.; Delavelle, J.; Henry, F.; Fasel, J.H. The Craniocervical Venous System in Relation to Cerebral Venous Drainage. *AJNR Am. J. Neuroradiol.* **2002**, *23*, 1500–1508.
39. Widjaja, E.; Griffiths, P.D. Intracranial MR Venography in Children: Normal Anatomy and Variations. *AJNR Am. J. Neuroradiol.* **2004**, *25*, 1557–1562.
40. Harloff, A.; Zech, T.; Wegent, F.; Strecker, C.; Weiller, C.; Markl, M. Comparison of Blood Flow Velocity Quantification by 4D Flow MR Imaging with Ultrasound at the Carotid Bifurcation. *AJNR Am. J. Neuroradiol.* **2013**, *34*, 1407–1413. [CrossRef]